Photochemistry of photosystem II reaction centre: Alternative electron pathways

Ph.D. thesis

Radek Litvín

Faculty of Science, University of South Bohemia
České Budějovice
2009

Supervisor: Doc. RNDr. František Vácha, CSc.

Litvín, R., 2009. Photochemistry of photosystem II reaction centre – Alternative electron donors. Ph.D. thesis, in English. – 67 p. Faculty of Science, University of South Bohemia, České Budějovice, Czech Republic.

Annotation
Properties of the electron transport chain within photosystem II reaction centre and PSII core complexes of peas were studied by differential VIS-NIR absorption spectroscopy and HPLC. A unique laboratory-built absorption spectrophotometer-fluorimeter is described.

Prohlašuji, že svoji disertační práci jsem vypracoval samostatně pouze s použitím pramenů a literatury uvedených v seznamu citované literatury.

Prohlašuji, že v souladu s § 47b zákona č. 111/1998 Sb. v platném znění souhlasím se zveřejněním své disertační práce, a to v úpravě vzniklé vypuštěním vyznačených částí archivovaných Přírodovědeckou fakultou elektronickou cestou ve veřejně přístupné části databáze STAG provozované Jihočeskou univerzitou v Českých Budějovicích na jejích internetových stránkách.

V Českých Budějovicích 20. ledna 2009

Radek Litvín

Acknowledgements

My foremost thanks belongs to Pavel Šiffel – the supervisor of my master's thesis, a very kind and thoughtful man, whom we have lost forever in the summer of 2003. He was a great teacher and scientist and even at present we often think and talk about him in the lab as if it was just a few minutes that he has left us. I would also like to thank František Vácha – my supervisor – without whom this work would have never materialized. He accepted to become my supervisor after the demise of Pavel Šiffel and despite being overwhelmed with work he has been very supportive and helped me overcome many obstacles.

My thanks also belong to all members of the Department of Photosynthesis of the Institute of Plant Molecular Biology, especially Ivana Hunalová and František Matoušek who prepared samples for my experiments. It has been fun working with the group.

My special thanks belong to my wife, Vlasta, who supported me in my decision to stay in school a little longer after obtaining a master's degree, and to our little Šárka. Both have been (and still are) the sun of my life.

Furthermore, I would also like to thank everyone who has not been mentioned above and supported me anyway.

Abbreviations

β-car	β-carotene
5chlRC	five-chlorophyll isolation of PSII RC
A	absorbance
ATP	adenosine triphosphate
car	carotenoid
CarD1, CarD2	β-carotene in D1, D2 protein, respectively
CCD	charge-coupled device, 2-dimensional light detector
Chl	chlorophyll
ChlD1, ChlD2	accessory chlorophylls of PSII RC located in D1, D2, respectively
Chl_Z^+	cation of one (or both) peripheral chlorophyll(s)
Chl_ZD1, Chl_ZD2	peripheral chlorophyll of D1, D2 proteins, respectively
CP26	minor antenna protein of photosystem II
CP29	minor antenna protein of photosystem II
CP43	core antenna protein of photosystem II
CP47	core antenna protein of photosystem II
cyt b_{559}	cytochrome b_{559} of PSII RC
D1, D2	psbA, psbB gene products
DM	n-dodecyl-β-D-maltoside
EPR	electron paramagnetic resonance
FeCy	potassium ferricyanide
HPLC	high performance liquid chromatography
LED	light emitting diode
LHCI	light-harvesting complex I
LHCII	light-harvesting complex II
MES	2-(N-morpholino)ethanesulfonic acid
NADPH	nicotinamide adenine dinucleotide phosphate
NIR	near-infrared part of the electromagnetic spectrum
OEC	oxygen evolving centre
P680	primary electron donor of photosystem II
PDA	photodiode array, 1-dimensional light detector
Pheo	pheophytin
PSII	photosystem II
PSII core	core of the photosystem II
PSII RC	photosystem II reaction centre (D1/D2/cyt b559/PsbI complex)
Q_A, Q_B	plastoquinones of photosystem II
SiMo	silicomolybdate
T–S	triplet-minus-singlet
UV	ultraviolet part of the electromagnetic spectrum
VIS	visible part of the electromagnetic spectrum

Contents

I Introduction

I.1 Photosynthesis

Photosynthesis is the sole source of energy for the vast majority of life on Earth. During photosynthesis the energy of light is converted into chemical energy of organic compounds. Alongside, in the most prominent oxygenic photosynthesis, inorganic carbon from carbon dioxide is bound and subsequently used to build plant bodies. Also, of special interest for all heterotrophs, molecular oxygen is released as a by-product. Photosynthesis is believed to be a very old biochemical pathway. Even the oldest known microbial life forms from around 3.5 billion years ago (Lepot et al. 2008, Allwood et al. 2006) are believed to be photosynthetic and they closely resemble today's cyanobacteria. This would of course mean that the evolution of photosynthesis as we know it today must have occurred very early during the dawn of life on Earth.

There are only two known general ways which life uses to capture the energy of light. An extremophile group of Halobacteria use light to pump protons and chloride ions across their cellular membrane. The respective proteins responsible for this are called bacteriorhodopsin and halorhodopsin. Their tertiary structures are similar to the rhodopsin (light-sensing pigment) found in vertebrate eye's retina (Lanyi 2004). Bacteriorhodopsin light utilization is not photosynthesis *sensu stricto* because there is no chemical synthesis occurring during bacteriorhodopsin action. The captured energy is stored in proton and chloride ion concentration differentials across cellular membranes.

The other way of capturing light energy by life or the "true" photosynthesis is found in a wide variety of organisms including flowering plants. It, in its "complete" form found in cyanobacteria and eukaryotic photosynthetic organisms, requires two light-driven enzymes called photosystems embedded in the specific cellular membrane (usually called the thylakoid membrane) alongside other protein complexes and a lot of water-soluble enzymes. Altogether, this ensemble captures light energy and uses it to produce ATP and NADPH which are then used to fixate carbon dioxide into sugar compounds and also to drive all other cellular processes. This complex process has been divided into so-called light-dependent reactions (which directly depend on light) and light-independent or dark reactions.

The light reactions produce ATP and NADPH and as a waste product release molecular oxygen (see fig.1 for a schematic of the light reactions). They happen on the thylakoid membrane, which is filled with dozens of photosystems and other enzymes, and in its close vicinity. The membrane assembly consists of photosystem II, cytochrome b_6f, plastocyanin, photosystem I, ferredoxin, ferredoxin-$NADP^+$ oxidoreductase and ATP synthase. The photosystem II catalyzes electron transfer from water to a membrane quinone molecule, which transports electrons towards cytochrome b_6f. This reaction is driven by the absorption of light. The electrons from water are then transported via cytochrome b_6f and plastocyanin to the photosystem I. Photosystem I catalyzes electron transfer from plastocyanin to ferredoxin with the help of light. The final step is an electron transport from ferredoxin to a final acceptor, $NADP^+$.

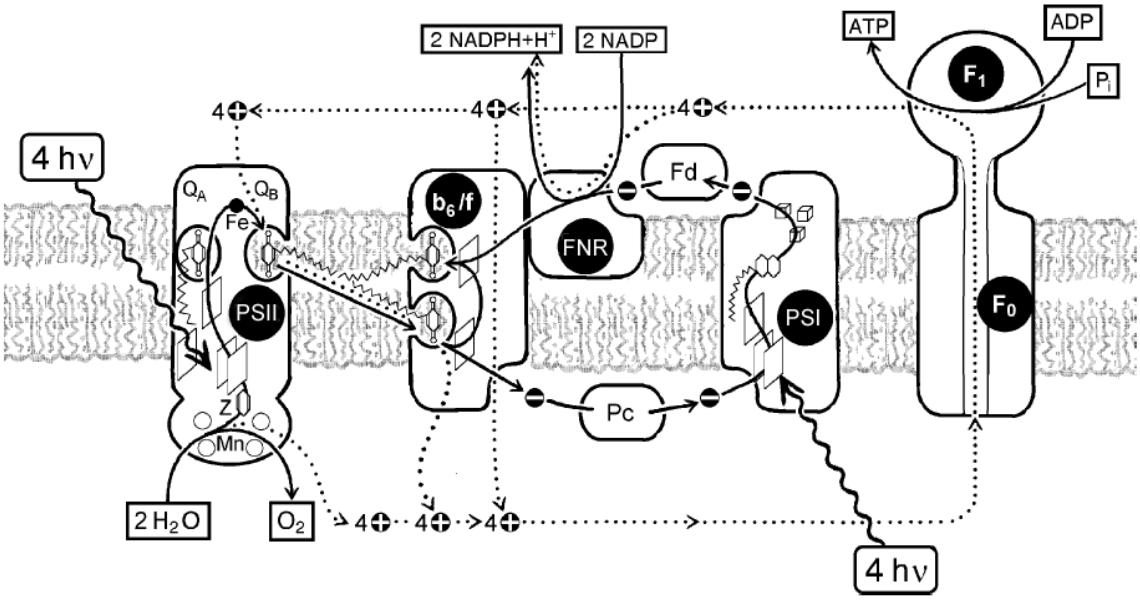

Fig.1: A schematic of the oxygenic photosynthesis thylakoid membrane. A basic stoichiometry of light-dependent reactions is also described. See text for details. Symbols: PSII – photosystem II; b_6/f – cytochrome b_6/f; FNR – ferredoxin-NADP$^+$ oxidoreductase; PSI – photosystem II; F_0, F_1 – subunits of the ATP synthase; Pc – plastocyanin; Fd – ferredoxin; hν – a photon; Q_A, Q_B – plastoquinones of PSII; Mn – manganese atoms of the oxygen evolving complex. Reprinted from Fyziologie rostlin. Šetlík, Seidlová, Šantrůček – a study material for the plant physiology course at the University of South Bohemia, located at http://kfar.bf.jcu.cz.

The whole pathway thus requires the absorption of two photons per one electron transported, one at photosystem II and one at photosystem I. A number of protons are transported across photosynthetic membrane alongside these electron transfer steps. The resulting differential in chemical potential of protons then drives ATP synthase which synthesizes ATP from ADP and inorganic phosphate.

In the dark reactions of photosynthesis ATP and NADH are used to drive fixation of carbon dioxide to five-carbon sugar called ribulose-1,5-bisphosphate creating two three-carbon molecules of glycerate-3-phosphate. This step is catalyzed by an enzyme called ribulose-bisphosphate carboxylase (often shortened to RuBisCO), which is arguably the most abundant protein on the Earth. In an intricate set of chemical reactions the three-carbon compounds are used to regenerate ribulose-1,5-bisphosphate and after six such cycles one new six-carbon sugar molecule is created.

As mentioned above the described machinery of photosynthesis is only found in cyanobacteria and eukaryotic photosynthetic organisms. Other organisms only “borrow” parts of it, constituting photosynthetic apparatus around photosystem I-like proteins (e.g. green sulphur bacteria) or around photosystem II-like proteins (e.g. purple bacteria). It is not clear whether the cyanobacterial system is the original one or whether it came together by joining the genetic information from type-I photosystem cell and type-II photosystem cell (Blankenship 2002). However, photosystems I and II have some structural homology and it is likely that they originated from a common ancestor protein. It is therefore probable that the sophisticated

cyanobacterial photosynthesis is the original one and the “partial” photosyntheses are derived from it by simplifying or omitting some parts.

The photosystems of the photosynthetic membrane are large complexes of protein subunits and cofactors. The cofactors include chlorophylls, pheophytins, carotenoids, quinones, hems, Fe-S clusters and iron, manganese and copper atoms. A photosystem can be functionally described to consist of an antenna(s) and a reaction centre. All electron transfer steps occur within a reaction centre whereas antennas are light concentrating devices which collect photon energy and funnel it towards the reaction centre. The antennas are described according to their location as peripheral or integral membrane complexes. Integral antennas can be either accessory or core (which are tightly connected to the reaction centres). Typical peripheral antenna examples are phycobilisomes found in cyanobacteria and red algae or chlorosomes found in green sulphur bacteria.

Green plants exclusively use integral membrane antennas. Photosystem I always contains core antenna which is integrated into the reaction centre proteins. Besides, photosystem I can also contain accessory antennas LHCI (LHC stands for light-harvesting complex) and LHCII. Photosystem II includes core antenna proteins CP43 and CP47 and may also be connected to LHCII.

Aside from concentrating light energy, antennas also regulate the amount of energy being delivered to the reaction centres. Two well known examples are the xanthophyll cycle and state transitions of LHCII. In the xanthophyll cycle the carotenoid violaxanthin is de-epoxided into zeaxanthin which has lower excited state energy and becomes an energy sink within the antenna. When light is no longer in excess a reverse process epoxides zeaxanthin back into violaxanthin. During state transition the LHCII antennas connect or disconnect to photosystem II or photosystem I and thus regulate their respective energy fluxes.

I.2 Photosystem II

The photosystem II (PSII) of green plants is a pigment-protein complex made up by about 25 proteins. *In vivo* it is most probably in dimeric form. However, these dimers may form even larger structures (Dekker and Boekema 2005). Photosystem II main components are the reaction centre (D1-D2-cyt b_{559} complex), oxygen evolving complex, inner antenna (main components are CP43 and CP47 proteins) and accessory antennas (LHCII, CP26 and CP29) (Barber et al. 1999). Several research groups succeeded in obtaining X-ray diffraction structures of PSII in the last years (Zouni et al. 2001, Kamiya and Shen 2003, Ferreira et al. 2004, Loll et al. 2005). The latest structure by Loll and co-workers is resolved to 3.0 Å resolution.

The LHCII is itself an assembly of several proteins. The complex is formed by a trimer of integral membrane proteins. A large number of pigments are bound to this protein scaffold. An isolated LHCII complex bounds 24 chlorophylls a (Chls a), 18 Chls b, three types of xanthophylls: 6 luteins, 3 neoxanthins and one violaxanthin (Kühlbrandt et al. 1994, Croce et al. 1999, Liu et al. 2005).

The core of the photosystem II (PSII core) is formed by a D1-D2-cyt b_{559} reaction centre, oxygen evolving complex, associated inner antennas CP43 and CP47 and a number of small subunits (Loll et al. 2005). The PSII core contains 35 Chls a (6 at the reaction centre, 13 at CP43 and 16 at CP 47) and 11 β-carotenes (β-car). Of the 11 β-car molecules, two are located within the reaction centre, three are at CP43 and five at CP47. Four of the inner antenna carotenoids are grouped together near the monomer-monomer boundary in PSII dimers. They are also very close to the D1-based carotene of the PSII reaction centre.

The oxygen evolving complex (OEC) is connected to the lumenal side of the PSII RC. It is responsible for donating electrons into the reaction centre. The OEC is formed in green plants by three small hydrophilic polypeptides weighing 17, 23 and 33 kDa. The main cofactors of the OEC are four manganese atoms, which are bound by amino acid side chains of the D1 protein (Ke 2001). The role of the OEC proteins is presumably stabilization of these atoms. Loss of the OEC proteins (particularly the 33 kDa one) causes the loss of the manganese atoms as well. Recently, it has been confirmed that these manganese atoms are associated with a calcium atom, forming a Mn_4Ca cluster (Loll et al. 2005). Electrons from the Mn_4Ca cluster are funnelled towards the primary donor of PSII by a redox-active tyrosine residue from D1 protein, denoted Tyr_Z or Y_Z. An analogical amino acid in the D2 polypeptide is presumably also redox-active but is probably not used for electron transport from the OEC.

The photosystem II reaction centre (PSII RC) is a complex of D1-D2-cyt b_{559}-psbI proteins which contains cofactors for electron transport. The PSII RC contains six chlorophylls a, two pheophytins, two β-carotenes, two quinones, one heme and one atom of iron. The spatial arrangement of cofactors within PSII RC is symmetrical, however only the pigments bound in D1 take part in the electron transport chain.

Two of the six Chl a molecules within PSII RC are very close together and form so-called special pair in analogy to the same entity found within purple bacteria PSII-type reaction centre. They used to be called the primary donor or P680 according to their red absorption maximum of 680 nm but currently it seems that not two but all four central Chls a form the primary donor. At physiological temperature all four central pigments of the PSII RC make contribution to the excited state. The contribution of the D1-based accessory chlorophyll is the largest and it is possible that charge separation is originated from this pigment. Following charge separation the positive charge is localized at the D1-based Chl of the special pair (Raszewski et al. 2008). A significant difference between $P680^+$ properties of PSII cores and PSII RC has been reported by Okubo et al. (2007). Contrary to the PSII cores, in PSII RC the positive charge is delocalized across the special pair which lowers its oxidation potential by ~0.1 V.

The two remaining chlorophylls of the PSII RC are called peripheral because of their location on the periphery of the RC. Their purpose seems to be funnelling excitation energy to the primary donor and possibly also photoprotection (see further). A schematic of the cofactor arrangement within PSII RC is plotted in fig.2.

The primary donor accepts excitation energy from the antenna complexes and as a result donates an electron to the primary acceptor, a pheophytin molecule within D1 protein which

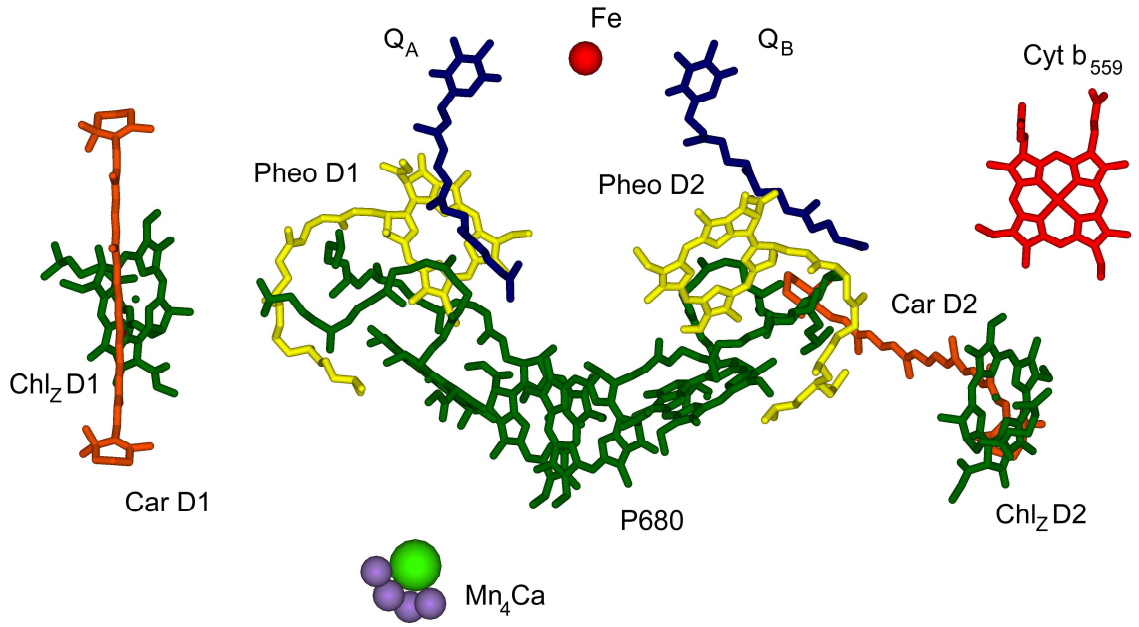

Fig.2: Arrangement of cofactors of the electron transport chain in the PSII reaction centre viewed along the membrane plane. Plotted from the data obtained by Loll et al. 2005. Color coding is as follows: chlorophylls – green; pheophytins – yellow; β-carotenes – orange; quinones – blue and heme – red. At the top, between the quinones, is an iron atom (red). Below the central group of chlorophylls (primary donor) is a Mn_4Ca cluster of oxygen evolving complex.

is located very close to the P680. The resulting charge separated state $P680^+Pheo^-$ is further stabilized by relocating the electron to the Q_A quinone molecule. The electron is further moved from the Q_A to the Q_B quinone. Oxidized primary donor is reduced by an electron originating from water. The quinone located in the Q_B pocket is capable of transporting two electrons at once so another photon needs to reach the primary donor to extract the second electron. When the Q_B quinone binds two electrons (and so it becomes a quinol) it is released from its binding pocket and another quinone is bound there. The doubly reduced quinone transports electrons towards the cytochrome b_6f complex.

As the $P680^+$ species is a very strong oxidant (estimated redox-potential of ~1.3 V, Rappaport et al. 2002) it can cause oxidative damage to PSII. This is unique among the various types of photosynthetic reaction centers because only PSII is capable of creating an oxidant strong enough to oxidize its own chlorophylls and carotenoids. Under conditions when the primary electron donation path is inhibited (i.e. in manganese depleted PSII or at low temperatures) alternate electron donors, including cyt b_{559}, peripheral chlorophylls and β-carotenes, can be photooxidized (reviewed by Frank and Brudvig 2004). It is also known that cyt b_{559} can be photoreduced by accepting electrons from Q_B (Buser et al. 1990). It is then possible that cyt b_{559} can participate in a cyclic electron transport within PSII (Allakhverdiev et al. 1997). In addition, photooxidized peripheral chlorophyll cations were shown to quench chlorophyll fluorescence (Schweitzer and Brudvig 1997). These processes (cyclic electron transport and/or excitation energy quenching) have been proposed to play a role under high

light or other stress conditions to protect the PSII reaction center from oxidative damage and photoinhibition (Stewart and Brudvig 1998). However, no assessment of in-vivo importance or extent of these processes has been done so far.

Because the edge-to-edge distance between cyt b_{559} and $P680^{+}$ is about 36 Å (Zouni et al. 2001, Kamiya and Shen 2003, Ferreira et al. 2004, Loll et al. 2005) the electron transfer is believed to occur via a redox intermediate. Such a distance is too large for rapid single step electron transfer. Redox active Car and/or Chl species appear to be the most probable candidates. Both Car and Chl photooxidation have been demonstrated in PSII core complexes from *Synechocystis, Synechococcus* and in PSII enriched spinach membranes at low temperatures (Faller et al. 2001, Telfer et al. 2003 and Tracewell and Brudvig 2003). However, the pathway(s) of electron transfer involving cyt b_{559}, Chl, and Car remains unclear, and both linear and branched pathways from cyt b_{559} to P680+ have been proposed.

Although it has been shown that β-carotene of PSII RC is able to quench singlet oxygen generated by triplet state of $P680^{*}$ (Telfer et al. 1994) it is probably not the only reason for its presence. It is known for more than twenty years that PSII RC-contained Car can be photooxidized (Schenck et al. 1982). Since then a number of efforts were made to elucidate attributes of this oxidation (latest: Hanley et al. 1999, Vrettos et al. 1999, Faller et al. 2001, Telfer et al. 2003, Noguchi et al. 1998, Tracewell and Brudvig 2003) employing VIS-NIR, Raman and EPR spectroscopy.

It is now generally believed that there are two spectrally and kinetically distinct β-carotene molecules in PSII RC. Their absorption maxima should be 507, 473 a 443 nm and 489, 458 a 429 nm (Telfer et al. 2003). Based on agreement of their LD spectra and their position within PSII crystal structure it is believed that the 507 nm-absorbing Car is located in the D2 protein and the other (489 nm-absorbing) is located in D1 (Tomo et al. 1997, Ishikita et al. 2007). The CarD1 is located between the Chl_ZD1 and P680, very close to the Chl_ZD1 (at a distance of 4.1 Å). The CarD2 is located in between the cyt b559 heme, Chl_ZD2 and ChlD2 of P680. The CarD1 has several β-carotene molecules of CP47 inner antenna in its proximity as opposed to the CarD2 which is more distant from other carotenes (Ishikita et al. 2007).

When oxidized, these Cars should have absorption maxima at 982 and 1027 nm according to Tracewell and Brudvig (2003) with the former decaying faster under cryogenic temperatures. The position of these NIR peaks differs slightly among organisms (observed on *Synechocystis*, *Synechococcus* and spinach) possibly indicating different protein environments and/or different quality of sample preparations. Observation of oxidized Car is usually accomplished by illumination of PSII cooled to ~20 K. The cyt b_{559} heme must be oxidized (e.g. by ferricyanide) prior to the freezing (Vrettos et al. 1999). Recently, a ~750 nm-absorbing β-car neutral radical has been spotted in PSII samples (Tracewell and Brudvig 2008).

Two symmetrically located peripheral chlorophylls (Chl_Z) are one of the major differences between PSII RC and purple bacterial rection centre. Photooxidation of chlorophyll other than P680 has been studied extensively since approximately 1985 (de Paula et al. 1985). This chlorophyll has been localized to one of the peripheral chlorophylls

coordinated by D1-His 118 and D2-His 117 (Chl_ZD1 and Chl_ZD2, respectively) based on the distance (39.5 ± 2.5 Å) of Chl_Z^+ from the PSII non-heme iron measured by saturation-recovery EPR (Koulougliotis et al. 1994) and on the distortion of the Chl_Z^+ resonance Raman spectra by site-directed mutations at D1-His 118 in *Synechocystis* 6803 (Stewart et al. 1998). However, another group located Chl_Z^+ to D2-His 117 (Wang et al. 2002). In addition, it has been announced that both Chl_ZD1 and Chl_ZD2 are oxidizable. Tracewell et al. (2001) report that in *Synechocystis* PSII core complexes they observed one NIR band at 814 nm, assigned to D1-His 118 based Chl_Z^+, but in spinach PSII membranes two Chl_Z^+ NIR bands were observed at 817 and 850 nm with the latter ascribed to Chl_ZD2^+. This is consistent with results of Hanley et al. (1999) who detected Chl_Z^+ NIR band at ~850 nm with a shoulder at ~820 nm upon illumination of PSII enriched membranes at 120 K. Both peripheral chlorophylls should have absorption maxima at 670 nm (Eijckelhoff et al. 1997, Schelvis et al. 1994, Allakhverdiev et al. 1997) although an effort is being employed to prove absorption maximum of Chl_ZD1 at 684 nm (Jankowiak et al. 1999).

It is well established that Chl_Z(s) can be irreversibly oxidized by illumination of ferricyanide-treated PSII or silicomolybdate-treated PSII RC at low temperatures (Telfer et al. 1990, Telfer et al. 1991, Vrettos 1999). Stewart et al. (2000) first reported reversibility of this oxidation by warming the sample to room temperature with 30 seconds being sufficient to rereduce Chl_Z^+ (in PSII core complexes). On the other hand Litvín (2003) observed rereduction half-time of about 200 seconds (in PSII RC).

Cytochrome b_{559} is an integral compound of PSII and it is necessary for succesful folding of PSII. It is composed as a heterodimer of α and β subunits containing one heme cofactor. Cyt b_{559} can be oxidized by illumination of PSII frozen below 100 K (Thompson and Brudvig 1988) or even at higher temperatures on Mn-depleted PSII (Stewart and Brudvig 1998). The rate constant for the photooxidation of cyt b_{559} in Mn-depleted PSII is ~50 s^{-1} (Buser et al. 1990) in contrast with rate constant in O_2-evolving PSII (~0.9 s^{-1}). It is often neccessary to prereduce cyt b_{559} (e.g. by ascorbate) because in many isolations it is oxidized (Buser et al. 1992). When cyt b_{559} is oxidized prior to low-temperature illumination, a Chl_Z is oxidized instead. Cyt b_{559} is presumed to have several redox forms and a typical sample of PS II contains a mixture of high-potential, intermediate-potential, and low-potential cyt b_{559} (Stewart and Brudvig 1998, Kaminskaya et al. 1999).

The sequence of reactions involving cyt b_{559}, Car, and Chl_Z in the secondary electron transfer pathways of PSII is not established. There is general agreement that β-carotene is the initial electron donor to $P680^+$ based on the observations that Car^+ is formed in highest yield at the lowest temperatures (4 K) and that the charge-separated state $Car^+Q_A^-$ decays by recombination at a faster rate than $Chl_Z^+Q_A^-$ (Tracewell et al. 2001).

The mechanism of cyt b_{559} and Chl_Z oxidation is not clear. Either both these cofactors communicate with $P680^+$ via Car (branched pathway) or cyt b_{559} has some other means of getting electron to $P680^+$ than Chl_Z, which is agreed to hand in electrons via Car molecule (parallel pathway). A branched pathway seems to be most likely based on both kinetic studies (Faller et al. 2001) and the locations of redox centers in the crystal structure (Loll et al. 2005).

The β-carotene identified in the D2 subunit of PSII by Ferreira et al. (2004) and Loll et al. (2005) is well positioned to transfer the electrons from cyt b_{559} or Chl_ZD2 to $P680^+$. When both Car and cyt b_{559} are prereduced only cytochrome oxidation is observed indicating that either transfer of electron via Car is ultrafast even at cryogenic temperatures or parallel pathway is the right one (Faller et al. 2001).

There are some recent hints that a broader view is necessary to fully understand the alternative electron pathways throughout the PSII RC. Ishikita and coworkers (Ishikita et al. 2007) calculated that the β-cars of the core antennas of PSII may form an efficient cation sink connected to the PSII RC (see fig.3 for an illustration of β-car positions within PSII). This theory seems to be confirmed in chapter IV of this thesis where we have found that in PSII core complexes the β-car photooxidation pathway is different than in PSII RC. Particularly

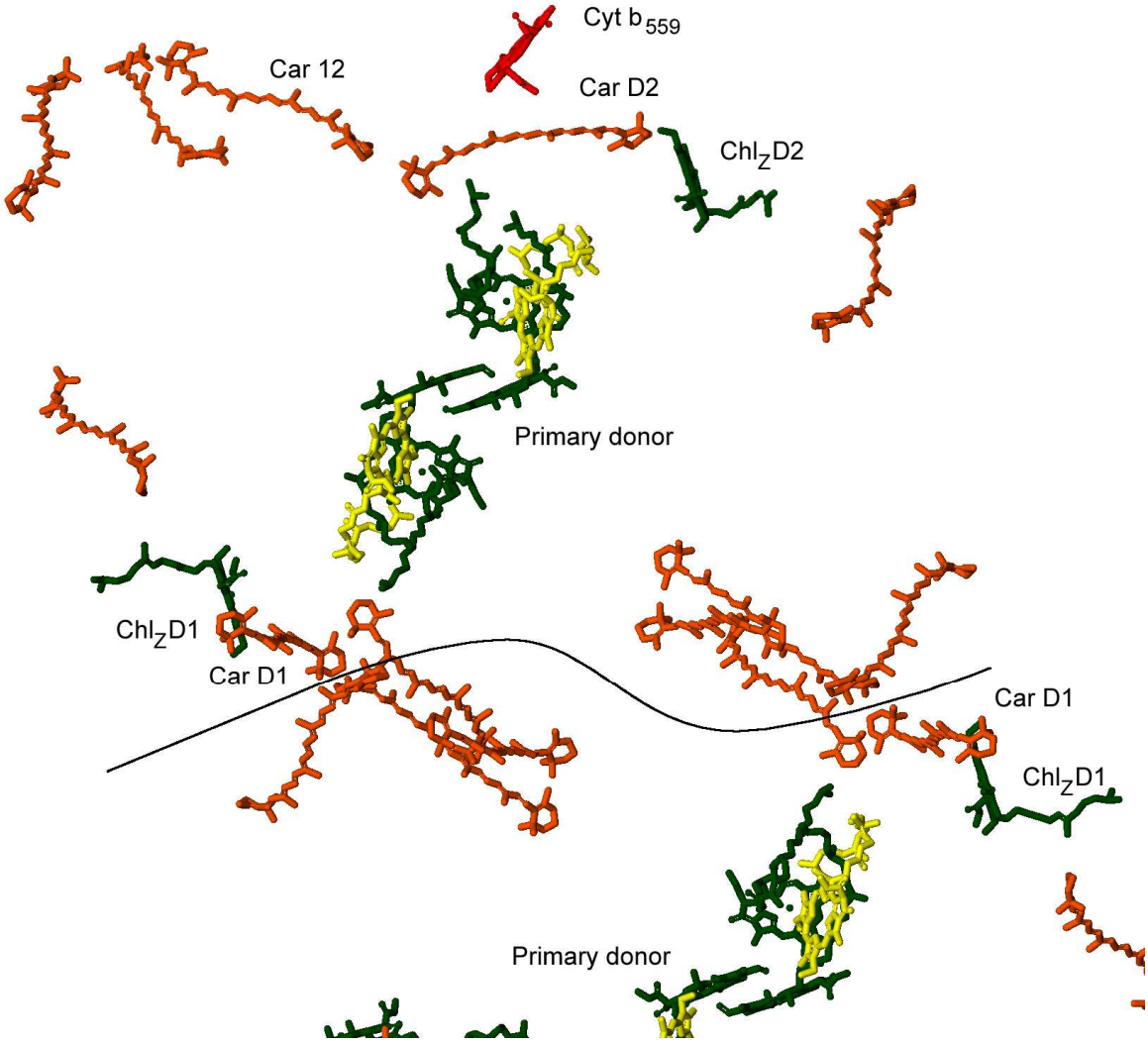

Fig.3: Cofactors within PSII core complex viewed perpendicular to the membrane plane. Only reaction centre porphyrins are shown. Color coding is as follows: chlorophylls – green; pheophytins – yellow; β-carotenes – orange, heme – red. Black line indicates approximate position of the monomer-monomer boundary within the PSII dimer. Plotted from the data obtained by Loll et al. (2005).

a novel carotene is formed in PSII RC but not in PSII cores. It was also proposed that the redox state of cyt b_{559} controls which secondary electron donors are favoured in PSII. A Car denoted Car 12 in the Loll et al. (2005) structure is pinpointed by Tracewell and Brudvig (2008) as a candidate for this switch of oxidation preference due to its proximity to the cyt b_{559} and also CarD2.

I.3 Outline of the thesis

The aims of this work were twofold. First, a testing of newly constructed kinetic spectrophotometer was conducted by experiments on a set of photosynthetic samples (chapters II and III). Second, an investigation of the properties of electron transport chain within PSII reaction centre was done mainly by means of this spectrophotometer (chapter IV).

Chapter II presents a newly developed multichannel spectrophotometer-fluorimeter with pulsed measuring light for measurements of light-induced absorbance changes in both transparent and scattering samples.

In chapter III, results of combined measurements of chlorophyll fluorescence and absorption spectroscopy of PSII reaction centres are presented.

Chapter IV describes a series of room temperature experiments to investigate the alternative electron donor pathways on PSII five-chlorophyll reaction centres and PSII core complexes.

An appendix (chapter VI) contains introduction to absorption spectroscopy and high performance liquid chromatography and additional technical information about the experimental apparatus used throughout this thesis.

I.4 References

Allakhverdiev SI, Klimov VV and Carpentier R (1997): Evidence for the involvement of cyclic electron transport in the protection of photosystem II against photoinhibition: influence of a new phenolic compound. Biochemistry 36, 4149-4154.

Allwood AC, Walter MR, Kamber BS, Marshall CP and Burch IW (2006): Stromatolite reef from the Early Archaean era of Australia. Nature 441, 714-718.

Barber J, Nield N, Morris EP and Hankamer B (1999) Subunit positioning in photosystem II revisited. Trends. Biochem. Sci. 24, 43-45.

Blankenship RE (2002): Molecular mechanisms of photosynthesis. Blackwell Science Ltd.

Buser CA, Thompson LK, Diner BA and Brudvig GW (1990): Electron-transfer reactions in manganese-depleted photosystem II. Biochemistry 29, 8977-8985.

Buser CA, Diner BA and Brudvig GW (1992): Photooxidation of cytochrome b559 in oxygen-evolving photosystem II. Biochemistry 31, 11449-11459.

Croce RR, Remelli C, Varotto JB and Bassi R (1999): The neoxanthin binding site of the major light harvesting complex (LHCII) from higher plants. FEBS Lett. 456, 1–6.

Dekker JP and Boekema EJ (2005): Supramolecular organization of thylakoid membrane proteins in green plants. Biochim. Biophys. Acta 1706, 12-39.

Eijckelhoff C, Vácha F, van Grondelle R, Dekker JP and Barber J (1997): Spectroscopic characterization of a 5 Chl a photosystem II reaction center complex. Biochim. Biophys. Acta 1318, 266-274.

Faller P, Pascal A and Rutherford AW (2001): β-carotene redox reactions in photosystem II: electron transfer pathway. Biochemistry 40, 6431-6440.

Ferreira KN, Iverson TM, Maghlaoui K, Barber J and Iwata S (2004): Architecture of the photosynthetic oxygen-evolving center. Science 303, 1831-1838.

Frank HA and Brudvig GW (2004): Redox functions of carotenoids in photosynthesis. Biochemistry 43, 8607-8615.

Hanley J, Deligiannakis Y, Pascal A, Faller P and Rutherford AW (1999): Carotenoid oxidation in photosystem II. Biochemistry 38, 8189-8195.

Ishikita H, Loll B, Besiadka J, Kern J, Irrgang K-D, Zouni A, Saenger W and Knapp E-W (2007) Function of two β-carotenes near the D1 and D2 proteins in photosystem II dimers. Biochim. Biophys. Acta 1767, 79-87.

Jankowiak R, Rätsep M, Picorel R, Seibert M, and Small G J (1999): Excited States of the 5-Chlorophyll Photosystem II Reaction Center. J. Phys. Chem. B 103, 9759-9769.

Kaminskaya O, Kurreck J, Irrgang KD, Renger G and Shuvalov VA (1999) Redox and spectral properties of cytochrome b_{559} in different preparations of photosystem II. Biochemistry 38, 16223–16235.

Kamiya N and Shen J-R (2003): Crystal structure of oxygen-evolving photosystem II from Thermosynechococcus vulcanus at 3.7 A resolution. PNAS 100, 98-103.

Ke B (2001): Photosynthesis: photobiochemistry and photobiophysics *in* Advances in Photosynthesis, series *ed.* Govindjee. Kluwer Academic Publishers.

Koulougliotis D, Innes JB and Brudvig GW (1994): Location of chlorophyll Z in photosystem II. Biochemistry 33, 11814-11822.

Kühlbrandt, W, Wang DN, and Fujiyoshi Y (1994): Atomic model of plant light-harvesting complex by electron crystallography. Nature 367, 614–621.

Lanyi JK (2004): Bacteriorhodopsin. Annual Review of Physiology 66, 665-688.

Lepot K, Benzerara K, Brown GE and Philippot P (2008): Microbially influenced formation of 2,724-million-year-old stromatolites. Nature Geoscience 1, 118-121.

Litvín R (2003): Study of the peripheral chlorophyll of the photosystem II reaction center; in Czech. Diploma thesis, Faculty of Biological Sciences, University of South Bohemia, České Budějovice, Czech Republic.

Liu Z, Yan H, Wang K, Kuang T, Zhang J, Gui L, An X and Chang W (2005): Crystal structure of spinach major light-harvesting complex at 2.72 Å resolution. Nature 428, 287-292.

Loll B, Kern J, Saenger W, Zouni A and Besiadka J (2005) Towards complete cofactor arrangement in the 3.0 angstrom resolution structure of photosystem II. Nature 438, 1040-1044.

Noguchi T, Tomo T and Inoue Y (1998): Fourier transform infrared study of the cation radical of the P680 in the photosystem II reaction center: evidence for charge delocalization on the chlorophyll dimer. Biochemistry 37, 13614-13625.

Okubo T, Tomo T, Sugiura M and Noguchi T (2007): Perturbation of the structure of P680 and the charge distribution on its radical cation in isolated reaction center complexes of Photosystem II as revealed by Fourier Transform Infrared Spectroscopy. Biochemistry 46, 4390-4397.

de Paula JC, Innes JB and Brudvig GW (1985): Electron transfer in photosystem II at cryogenic temperatures. Biochemistry 24, 8114-8120.

Rappaport F, Guergova-Kuras M, Nixon PJ, Diner BA and Lavergne J (2002): Kinetics and pathways of charge recombination in photosystem II. Biochemistry 41, 8518-8527.

Raszewski G, Diner BA, Schlodder E and Renger T (2008) Spectroscopic properties of reaction center pigments in photosystem II core complexes: revision of the multimer model. Biophys. J. 95, 105-119.

Schelvis JPM, van Noort PI, Aartsma TJ and van Gorkom HJ (1994): Energy transfer, charge separation and pigment arrangement in the reaction center of Photosystem II. Biochim. Biophys. Acta 1184, 242-250.

Schenck CC, Diner BA, Mathis P and Satoh K (1982): Flash-induced carotenoid radical cation formation in photosystem II. Biochim. Biophys. Acta 680, 216-227.

Schweitzer RH and Brudvig GW (1997): Fluorescence quenching by chlorophyll cations in photosystem II. Biochemistry 36, 11351-11359.

Stewart DH and Brudvig GW (1998): Cytochrome b_{559} of photosystem II. Biochim. Biophys. Acta 1367, 63-87.

Stewart DH, Cua A, Chisholm DA, Diner BA, Bocian DF and Brudvig GW (1998): Identification of histidine 118 in the D1 polypeptide of photosystem II as the axial ligand to chlorophyll Z. Biochemistry 37, 10040-10046.

Stewart DH, Nixon PJ, Diner BA and Brudvig GW (2000): Assignment of the Q_y Absorbance Bands of Photosystem II Chromophores by Low-Temperature Optical Spectroscopy of Wild-Type and Mutant Reaction Centers. Biochemistry 2000, 39, 14583-14594.

Telfer A, Durrant J and Barber J (1990): Transient absorption spectroscopy of the primary electron donor, P680, in the isolated Photosystem II reaction centre. Biochim. Biophys. Acta 1018, 168-172.

Telfer A, De Las Rivas J and Barber J (1991): Beta-carotene within the isolated Photosystem II reaction centre: photooxidation and irreversible bleaching of this chromophore by oxidised P680. Biochim. Biophys. Acta 1060, 106-114.

Telfer A, Dhami S, Bishop SM, Phillips D and Barber J (1994): β-carotene quenches singlet oxygen formed by isolated photosystem II reaction centers. Biochemistry 33, 14469-14474.

Telfer A, Frolov D, Barber J, Robert B and Pascal A (2003): Oxidation of the two β-carotene molecules in the photosystem II reaction center. Biochemistry 42, 1008-1015.

Thompson LK and Brudvig GW (1988): Cytochrome b-559 may function to protect photosystem II from photoinhibition. Biochemistry 27, 6653-6658.

Tomo T, Mimuro M, Iwaki M, Kobayashi M, Shigeru I and Satoh K (1997) Topology of pigments in the isolated photosystem II reaction center studied by selective extraction. Biochim. Biophys. Acta 1321, 21-30.

Tracewell CA, Cua A, Stewart DH, Bocian DF and Brudvig GW (2001): Characterization of carotenoid and chlorophyll photooxidation in photosystem II. Biochemistry 40, 193-203.

Tracewell CA, Brudvig GW (2003): Two redox-active beta-carotene molecules in photosystem II. Biochemistry 42, 9127-9136.

Tracewell CA and Brudvig GW (2008): Characterization of the secondary electron-transfer pathway intermediates of photosystem II containing low-potential cytochrome b_{559}. Photosynth. Res. DOI 10.1007/s11120-008-9360-8.

Vrettos JS, Stewart DH, de Paula JC and Brudvig GW (1999): Low-temperature optical and resonance Raman spectra of a carotenoid cation radical in photosystem II. J. Phys. Chem. B 103, 6403-6406.

Wang J, Gosztola D, Ruffle SV, Hemann C, Seibert M, Wasielewski MR, Hille R, Gustafson TL and Sayre RT (2002): Functional Asymmetry of Photosystem II D1 and D2 Peripheral Chlorophyll Mutants of Chlamydomonas Reinhardtii. PNAS USA 99, 4091-4096.

Zouni A, Witt H-T, Kern J, Fromme P, Krauß N, Saenger W and Orth P. (2001): Crystal structure of photosystem II from Synechococcus elongatus at 3.8 A resolution. Nature 409, 739-743.

II New multichannel kinetic spectrophotometer-fluorimeter with pulsed measuring beam for photosynthesis research

This chapter was published in the journal Photosynthesis Research:

Bína D, Litvín R, Vácha F and Šiffel P (2006): New multichannel kinetic spectrophotometer–fluorimeter with pulsed measuring beam for photosynthesis research. Photosynth. Res. 88: 351-356.

II.1 Abstract

A multichannel kinetic spectrophotometer–fluorimeter with pulsed measuring beam and differential optics has been constructed for measurements of light-induced absorbance and fluorescence yield changes in isolated chlorophyll-proteins, thylakoids and intact cells including algae and photosynthetic bacteria. The measuring beam, provided by a short (2 μs) pulse from a xenon flash lamp, is divided into a sample and reference channel by a broad band beam splitter. The spectrum in each channel is analyzed separately by a photodiode array. The use of flash measuring beam and differential detection yields high signal-to-noise ratio (noise level of 2×10^{-4} in absorbance units per single flash) with negligible actinic effect. The instrument covers a spectral range between 300 and 1050 nm with a spectral resolution of 2.1, 6.4 or 12.8 nm dependent on the type of grating used. The optical design of the instrument enables measuring of the difference spectra during an actinic irradiation of samples with continuous light and/or saturation flashes. The time resolution of the spectrophotometer is limited by the length of Xe flash lamp pulses to 2 μs.

Překlad abstraktu:

Zkonstruovali jsme mnohokanálový kinetický spektrofotometr-fluorimetr s pulsním měřicím svazkem a diferenciální optikou pro měření světlem indukovaných změn absorpce a fluorescence v izolovaných chlorofylových proteinech, tylakoidech a intaktních buňkách včetně řas a fotosyntetických bakterií. Měřicí svazek, poskytovaný krátkým (2 μs) pulsem xenonové výbojky, je rozdělen širokopásmovým děličem svazků do vzorkového a referenčního kanálu. Spektrum každého kanálu je samostatně analyzováno řadou fotodiod. Použití pulzního měřicího svazku a diferenciální detekce zajišťují vysoký poměr signál/šum (šum činí 2×10^{-4} absorpčních jednotek na jeden záblesk) se zanedbatelným aktinickým efektem. Přístroj pokrývá spektrální oblast 300 – 1050 nm se spektrálním rozlišením 2.1, 6.4 nebo 12.8 nm v závislosti na použité difrakční mřížce. Optický design přístroje umožňuje měření rozdílových spekter v průběhu aktinického ozáření vzorků prostřednictvím kontinuálního nebo pulsního světla. Časové rozlišení spektrofotometru je limitováno délkou pulsů xenonové lampy na 2 μs.

Autorský podíl:

Radek Litvín má na publikaci podíl 30%.

III Conformational changes and their role in non-radiative energy dissipation in photosystem II reaction centres

This chapter was published in the journal Photochemical and Photobiological Sciences:

Litvín R, Bína D, Šiffel P and Vácha F (2005): Conformational changes and their role in non-radiative energy dissipation in photosystem II reaction centres. Photochem. Photobiol. Sci. 4: 999-1002.

III.1 Abstract

Accumulation of reduced pheophytin in photosystem II under illumination at low redox potential is known to be accompanied by a pronounced decrease of a chlorophyll fluorescence yield. Simultaneous measurement of this fluorescence quenching and absorbance changes in photosystem II reaction centres, in the presence of dithionite, showed each event to have different temperature dependence. While fluorescence quenching was suppressed more than 20 times when measured at 77 K, pheophytin accumulation decreased only 5 times. At 77 K, the fluorescence was quenched considerably, but only in those reaction centres where reduced pheophytin had been accumulated at room temperature before sample freezing. This showed that the accumulation of reduced pheophytin above 240 K was accompanied by an additional, most probably conformational, change in the reaction centre that substantially enhanced non-radiative dissipation of excitation energy.

Překlad abstraktu:

Je známo, že akumulace redukovaného feofytinu v osvětleném fotosystému II za nízkého redox potenciálu je provázena významným poklesem výtěžku fluorescence chlorofylu. Simultánní měření tohoto zhášení fluorescence a absorpčních změn v reakčních centrech fotosystému II v přítomnosti dithionitu ukázala rozdílnou teplotní závislost těchto dvou jevů. Zatímco zhášení fluorescence bylo při 77K potlačeno vice než dvacetkrát, akumulace feofytinu poklesla pouze pětkrát. Při 77K byla fluorescence významně zhášena pouze v reakčních centrech, kde byl redukovaný feofytin akumulován při pokojové teplotě před zmrazením vzorku. To ukazuje, že akumulace redukovaného feofytinu při teplotě přes 240K je provázeno další, pravděpodobně konformační, změnou v reakčním centru, která významně zvyšuje míru nezářivé disipace excitační energie.

Autorský podíl:

Radek Litvín je prvním autorem článku, jeho podíl činí 30%.

IV Room temperature photooxidation of β-carotene and peripheral chlorophyll in photosystem II reaction centre

This chapter was published in the journal Photosynthesis Research:

Litvin R, Bina D and Vacha F (2008): Room temperature photooxidation of β-carotene and peripheral chlorophyll in photosystem II reaction centre. Photosynth. Res. 98: 179-187.

IV.1 Abstract

Differential kinetic absorption spectra were measured during actinic illumination of photosystem II reaction centres and core complexes in the presence of electron acceptors silicomolybdate and ferricyanide. The spectra of samples with ferricyanide differ from those with both ferricyanide and silicomolybdate. Near-infrared spectra show temporary β-carotene and peripheral chlorophyll oxidation during room temperature actinic illumination. Peripheral chlorophyll is photooxidized even after decay of β-carotene oxidation activity and significant reduction of β-carotene content both in reaction centres and photosystem II core complexes. Besides, new carotenoid cation is observed after about 1 s of actinic illumination in the reaction centres when silicomolybdate is present. Similar result was observed in PSII core complexes. HPLC analyses of illuminated reaction centres reveal several novel carotenoids whereas no new carotenoid species were observed in HPLC of illuminated core complexes. Our data support the proposal that pigments of inner antenna are a sink of cations originating in the photosystem II reaction centre.

Překlad abstraktu:

Měřili jsme diferenciální kinetická absorpční spektra reakčních center a core komplexů fotosystému II v průběhu aktinického osvětlení v přítomnosti elektronových akceptorů silikomolybdátu a ferrikyanidu. Spektra vzorků s ferrikyanidem se liší od spekter vzorků s ferrikyanidem a silikomolybdátem. Blízká infračervená spektra ukazují dočasnou oxidaci β-karotenu a periferního chlorofylu v průběhu aktinického osvětlení za pokojové teploty. Periferní chlorofyl je fotooxidován i po vymizení oxidovatelnosti β-karotenu a podstatném snížení obsahu β-karotenu v reakčních centrech i v core komplexech fotosystému II. Krom toho byl po cca 1 s aktinického ozáření pozorován nový karotenoidový kation v reakčních centrech pokud byl přítomen silikomolybdát. Obdobné výsledky byly pozorovány v core komplexech fotosystému II. HPLC analýzy osvětlených reakčních center odhalily několik nových karotenoidů v reakčních centrech a žádné nové karotenoidy v core komplexech. Naše data podporují tezi, že pigmenty vnitřní antény jsou jímkou kationů pocházejících z reakčního centra fotosystému II.

Autorský podíl:

Radek Litvín je první autor publikace, jeho podíl činí 80%.

V Summary

Photosystem II is the place where photosynthesis, one of the most important chemical reactions on Earth, starts. Moreover, it is also the place where electrons are extracted from water and molecular oxygen is released; a fact vital to all heterotrophs on Earth. To achieve this feat the photosystem II possesses very powerful machinery, particularly the primary electron donor. This work used mainly absorption spectroscopy to study mechanisms which regulate energy flows through the photosystem II reaction centre and prevent damage to it by unquenched primary donor cation.

Chapter II describes a new multichannel kinetic absorption spectrophotometer which is sensitive enough to capture unrepeatable absorption transients and has fully customizable measuring sequences. It also makes it possible to simultaneously detect changes in absorbance and fluorescence emitted from the sample.

In chapter III, PSII reaction centre structural change caused by pheophytin reduction is described based on measurements of absorbance and fluorescence yield at room and cryogenic temperatures. This structural change enhances non-radiative energy dissipation of the excitation energy within PSII reaction centre.

In chapter IV, new data on the role of peripheral chlorophyll and β-carotene in the PSII reaction centre were presented. These alternative electron donors within PSII reaction centre were observed operating at room temperature. The most important conclusion is that unique, non-repeatable processes occur during experiments. In PSII RC the primary donor irreversibly oxidises the β-carotene to a new undefined carotenoid. The presence of this process is described for the first time in this thesis due to the potential of the new multichannel kinetic absorption spectrophotometer avoiding the usual procedure of averaging many repeated illuminations of the sample.

VI Appendix

VI.1 Absorption spectroscopy

Many of the cofactors forming the electron transport chain in photosynthetic organisms absorb visible light which makes it possible to study them by using visible light absorption spectroscopy. During absorption of a quantum of electromagnetic radiation (a photon) by a molecule or atom the quantum is destroyed and an electron from the absorbing substance is excited to the higher-energy level. The energy of the absorbed photon has been transformed into the potential energy of the excited electron. Whether a photon is absorbed by a molecule or not depends (among other things) on the state of the valence electrons of this molecule. Molecules in ground state differ in their absorption properties from the same molecules whose valence electrons have undergone a change either by oxidization or reduction or by excitation to the higher orbitals because each of these states has different energy level structure which determines absorption properties.

Absorbance is simply measured by comparing the intensity of light which passed through the sample with the intensity of light which passed through identical path except the sample (so-called reference beam). Absorbance is then defined as:

$$A = -log_{10}\frac{I_1}{I_0}$$

Where I_1 is the intensity of light in the sample path and I_0 the same value for the reference path. These readings can be taken by using the same light path through manually exchanging sample and reference cuvettes but most spectrometers today have separate chambers for sample and reference readings which speeds-up the processing.

The absorbance is related to the absorbing species concentration according to eq. 2 which links together material constant ε (molar decadic absorption coefficient), optical path length l and sample concentration c.

$$A = \varepsilon.l.c$$

The absorption coefficient, ε, is a wavelength-specific parameter because generally the ability to absorb given photon depends upon its wavelength. A record of absorption of a given sample according to the wavelength (or frequency) of incident light is called the absorption spectrum (see fig.1 for an example of the absorption spectrum of photosynthetic sample).

There are a number of requirements to be followed during absorbance readings. Unfortunately many of them are not possible to comply with during photosynthesis experiments due to the nature of the objects studied.

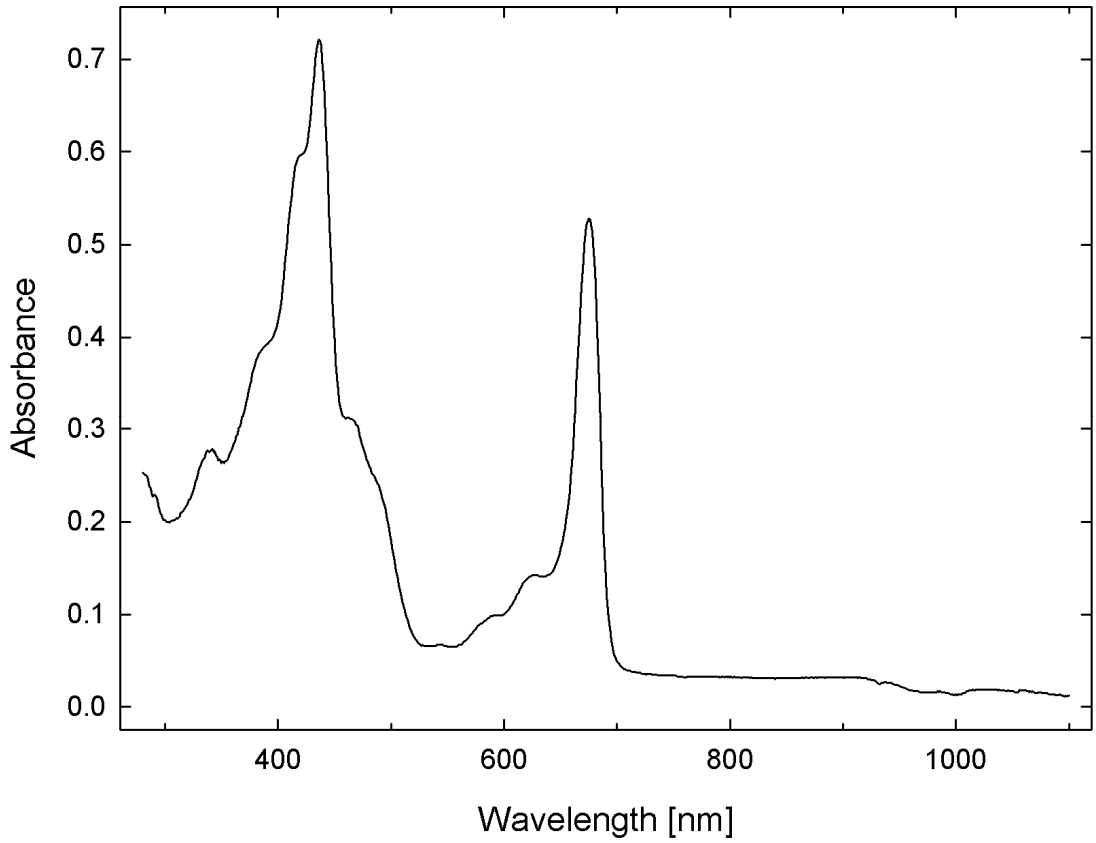

Fig.1: Absorption spectrum of PSII core complexes. Note pronounced absorption peaks in the blue (below 500 nm) and red (600 nm – 700 nm) parts of the spectrum. Green light (500 – 550 nm) is absorbed very little which gives all plants a characteristic green colour. No significant absorption can be seen above 700 nm which greatly facilitates absorption experiments in this area on dense samples.

The absorbing units within the sample must act independently of each other. This is certainly not true in photosynthetic proteins where a precise alignment of cooperating pigments is present. This usually does not interfere significantly with the measurement but in some cases physical regrouping of these pigments or whole proteins changes macroscopic absorption properties significantly.

The sample should be optically homogeneous. This is true for isolated pigment-protein complexes but whole chloroplasts or bacteria cells form very turbid sample which increases apparent absorbance and makes measuring these samples more demanding because a lot of light is lost by scattering. The absorption spectra of such samples are also distorted due to the fact that shorter wavelength (blue) light is scattered more than longer wavelength (red) light.

The sample should not be influenced by the measuring light beam. This is very difficult to achieve in photosynthetic samples because these are by definition very well developed to catch the maximum available amount of light and store as much of its energy as possible in a useful form. Following illumination the sample changes its configuration (e.g. a quinone is reduced or some pigment is oxidized) and therefore also its absorbance is changed. This effect

can only be mitigated by using the lowest possible measuring beam intensity. Low measuring beam intensity worsens the signal-to-noise ratio which is often detrimental to the quality of obtained data. Actinic effect of the measuring light creates the most significant trade-off during experiments on photosynthetic samples. One has to be reasonably sure that the measuring light does not significantly interfere with the sample measured or, at least, account for this effect when interpreting these data.

Lastly, the photosynthetic samples containing chlorophyll are well known to emit fluorescence when illuminated. This lowers measured absorbance by adding fluorescent photons to those from the measuring beam. Appropriate design of the spectrometer and filtering may make this effect negligible. Photons spontaneously emitted from the sample propagate in random directions. Thus, the farther the detector is located from the sample the smaller amount of fluorescence is detected. The spectrometer described in chapter II of this thesis currently collects light of the measuring beam by a 3 cm mirror positioned approximately 12 cm from the sample. This way the amount of detected fluorescence is lowered to less than 0.5 % of the original (all-directional) intensity. Despite this an effect of very powerful actinic light has to be accounted for by reading-out the detector with only actinic light (no measuring light) triggered. An example of chlorophyll fluorescence passing through to the detector is shown in appendix section 7.

An absorption spectrometer is typically made up of a light source, sample and reference compartments and a detector unit. Most light sources used in spectrometers provide polychromatic (white) light which unmodified is not useful for absorbance measurement. A dispersive element (usually a diffraction grating) is put into the measuring light path to disperse the light beam into a spectrum.

Depending on the position of the dispersion grating versus the sample chamber two types of spectrometers can be distinguished. A single-channel spectrometer has the grating in front of the sample. In such alignment a relatively narrow spectrum (theoretically monochromatic) light illuminates the sample and is detected by single channel detector. An advantage of such design is low sample illumination – monochromatic light of relatively low intensity is used. Another advantage is the relatively simple to produce single-channel detector. The disadvantage is the need to provide with the rotating grating for different wavelength readings which adds engineering complexity and increases cost. Measuring the whole spectrum may take a lot of time although there are instruments which manage to deal with this problem successfully (see e.g. Olis, Inc., http://www.olisweb.com/).

In a multichannel spectrometer the diffraction grating is positioned behind the sample so the white light beam illuminates the sample and it is dispersed afterwards. A multichannel detector such as a CCD or photodiode array (PDA) is used. Such detectors make it possible to measure entire spectrum in a short time at the expense of higher complexity and cost. The spectrum read-out time is essentially limited by the length of light pulse required to achieve good signal-to-noise ratio. Shorter measuring times must be compensated by more intense measuring light which may cause problems because such light often causes significant change

to the sample. This is even more pronounced than in single-channel spectrometer because the measuring beam passing through the sample is polychromatic.

Many changes observed within the photosynthetic apparatus only concern a few of the pigments present. Differential absorption spectra are often used instead of just a sequence of "normal" absorption spectra to help in visualisation of these small changes. For example a pheophytin molecule from PSII RC changes significantly its absorption when reduced by an electron from the primary donor. Because only one pheophytin is reduced per reaction centre only a small part of the overall absorption is changed even if we manage to reduce pheophytins in all of the RCs present in the sample. A differential spectrum discards the underlying absorption and only considers the change and therefore provides a very nice way of showing what happened in the sample (see fig.2 for an example of pheophytin differential absorption spectrum).

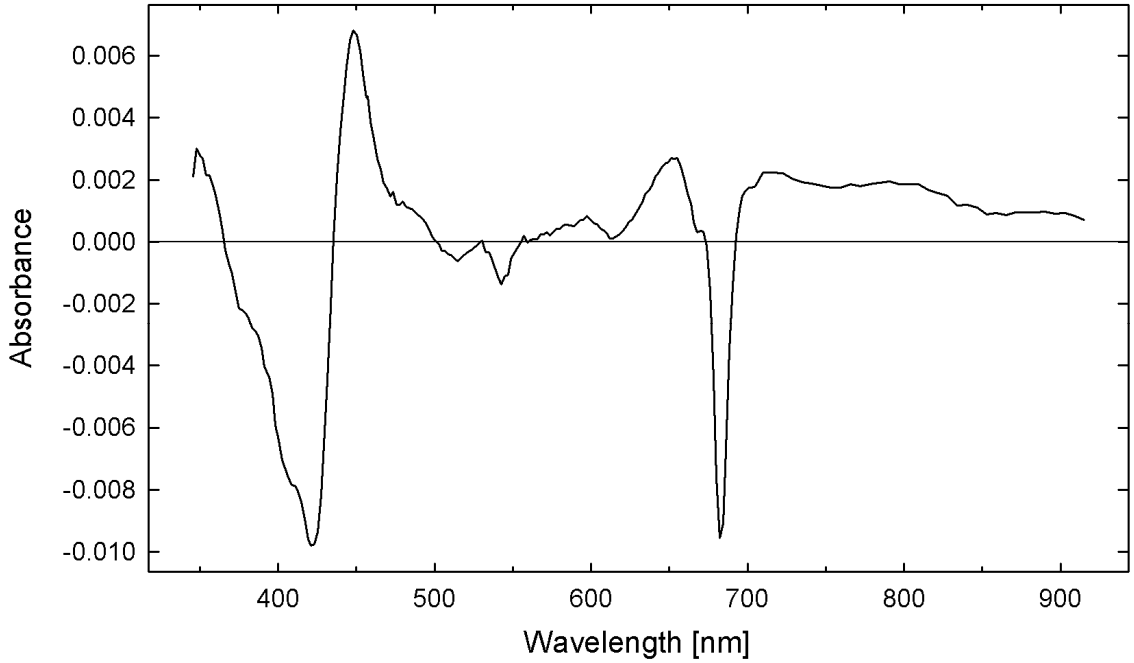

Fig.2: An example of differential absorption spectrum – light-minus-dark spectrum of PSII reaction centre with an electron donor (dithionite). At first a spectrum of dark-adapted sample was measured then actinic illumination was applied and after a couple of seconds another spectrum was measured. The dark spectrum was then subtracted from the second spectrum. The spectrum is negative where the sample lost absorption and positive where new absorption bands arose. In this particular case a reduced pheophytin ($Pheo^-$) is accumulated by actinic light. It is identifiable by losing characteristic ground-state absorption at 545 nm. Note very low absorbance changes on a sample with absorption very similar to that in fig.1. The absorbance change at 682 nm of ~0.01 A is approximately 2 % of the original absorbance ~0.5 A.

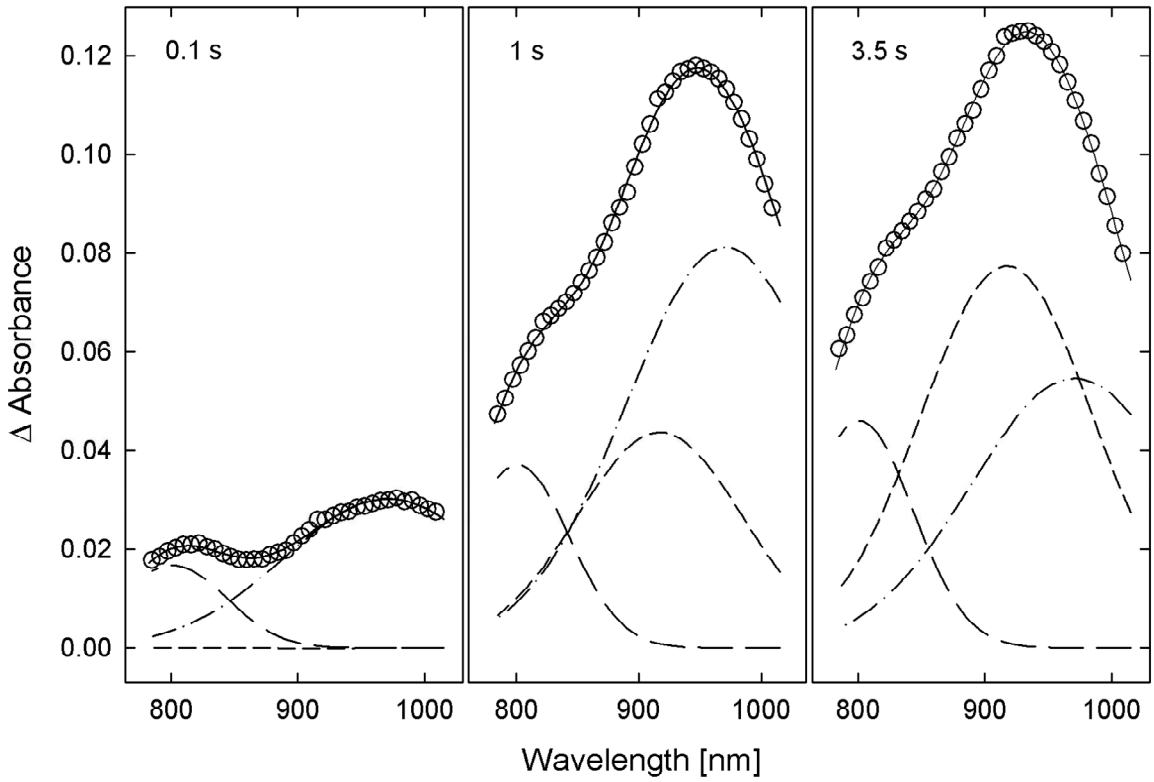

Fig.3: An illustration of global gaussian fitting on absorption spectra. PSII RCs were illuminated in the presence of electron acceptors and a series of spectra was measured. A snapshot of three individual spectra from this experiment is shown. Delays after turning on the actinic light are indicated. The whole dataset was used to globally fit a sum of three gaussian profiles. Measured data points are plotted as circles, fitted function is plotted as line. Individual fitted gaussians at positions 801 nm (long dash), 917 nm (short dash) and 971 nm (dash-dot) are also shown. If processed individually these spectra could be reasonable fitted with just two gaussian functions (which would be different in each spectrum).

VI.2 Absorption spectra processing

It is rarely the case that only one pigment is changed in the sample during the experiment. Often at least two absorbing species take part in action during an experiment with photosynthetic material. If that is the case the measured difference absorption spectra may be very difficult to decipher. One should in ideal case be able to obtain concentrations of all states of all pigments observed during the experiment. This is however often not possible because the pigments have overlapping absorption spectra or their kinetics are very similar.

In chapter IV we have used a very simple approach to separate spectra of the individual participating species. In the near infrared part of the absorption spectrum many of the pigments have spectra which are relatively similar to a simple gaussian profile. We have taken all of the spectra measured during one experiment and run a so called global fitting procedure. Global fitting is mathematically identical to the commonly known minimizing algorithms but the input data are a bit different. A common approach is to prepare a two-dimensional data (e.g. absorbance versus wavelength data) and fit a model onto it. In global fitting the input

data are three dimensional (e.g. absorbance versus wavelength at different times from the onset of experiment). To lower the number of unknown parameters some of them are shared among all two-dimensional parts of the dataset. In the case of the gaussian profiles the position and width parameters were shared among all spectra. This is possible because these parameters are not expected to change during experiment (i.e. along the time dimension of the dataset). This way the number of unknown parameters in 47 spectra was lowered from 470 to 194[1]. This increased the stability of the fitting procedure by providing more data points per unknown parameter. See figure 3 for an example of results obtained from the global-fitted data.

$$y = a.exp\left(-\frac{1}{2}\left(\frac{x-\mathbf{x_0}}{\mathbf{b}}\right)^2\right)$$

A gaussian profile function. Parameter description: a – peak amplitude; x_0 – position of the maximum on the x axis; b – relates to the width of the profile. Parameters shared during global fitting (x_0 and

VI.3 High performance liquid chromatography

High performance liquid chromatography (HPLC) is a common analytical tool used widely by biochemical laboratories to identify, quantify and separate molecules. In HPLC the molecules are separated by moving across the stationary phase. Separation is achieved by interaction of sample molecules with the stationary phase. The stationary phase consists of small particles (typically ~ 5 μm diameter) filled within a column. The sample is injected into the mobile phase flow driven by a pump through the column to the detector. Smaller particles of stationary phase have larger surface area which is beneficial for the quality of separation but also requires better pumps because higher pressure is required to pump the mobile phase through the column at specified flow rate.

The delay between sample injection and compound elution from the HPLC column is called retention time and it is specific for each compound. The retention time depends upon interactions between the stationary phase, molecules analyzed and mobile phase. The higher the affinity of the molecule to the stationary phase the longer it takes it to pass through the column. Resolution of similar compounds is improved by longer time spent in interaction with the stationary phase. This can be achieved by using smaller fill particles, longer columns or slower flow through the column.

In reversed-phase HPLC non-polar hydrocarbon chains are covalently bonded to the particles within the column. For example a column with designation C_{18} has eighteen carbon long chains on the surface of the column fill. Such stationary phase is therefore non-polar and a more polar solvent (mobile phase) is used. The most polar compounds from the sample are eluted first because their interaction with the stationary phase is the weakest. Less polar

[1] We have been fitting three gaussian functions plus offset per each spectrum. Each gaussian profile has three parameters – position, width and amplitude. This gives 47 spectra × (3 gaussians × 3 parameters + 1 offset) = 470. In the case of global fitting two of the three gaussian parameters were shared – position and width. This gives 47 spectra × (3 gaussians × 1 parameter + 1 offset) + 3 gaussians × 2 shared parameters = 194.

compounds are eluted as last e.g. in chapter IV the β-carotene is the last to come out of the column because it is very non-polar in the context of PSII RC pigments.

The last machine in the assembly of HPLC is the detector. In many setups this is a simple single- or multichannel UV/VIS absorption detector which is useful for identifying coloured samples or compounds which absorb in the ultraviolet parts of the spectrum like proteins. In other setups the detector may be a mass spectrometer which identifies compounds based on their molecular masses.

VI.4 Spectrum of the measuring Xe lamp pulse

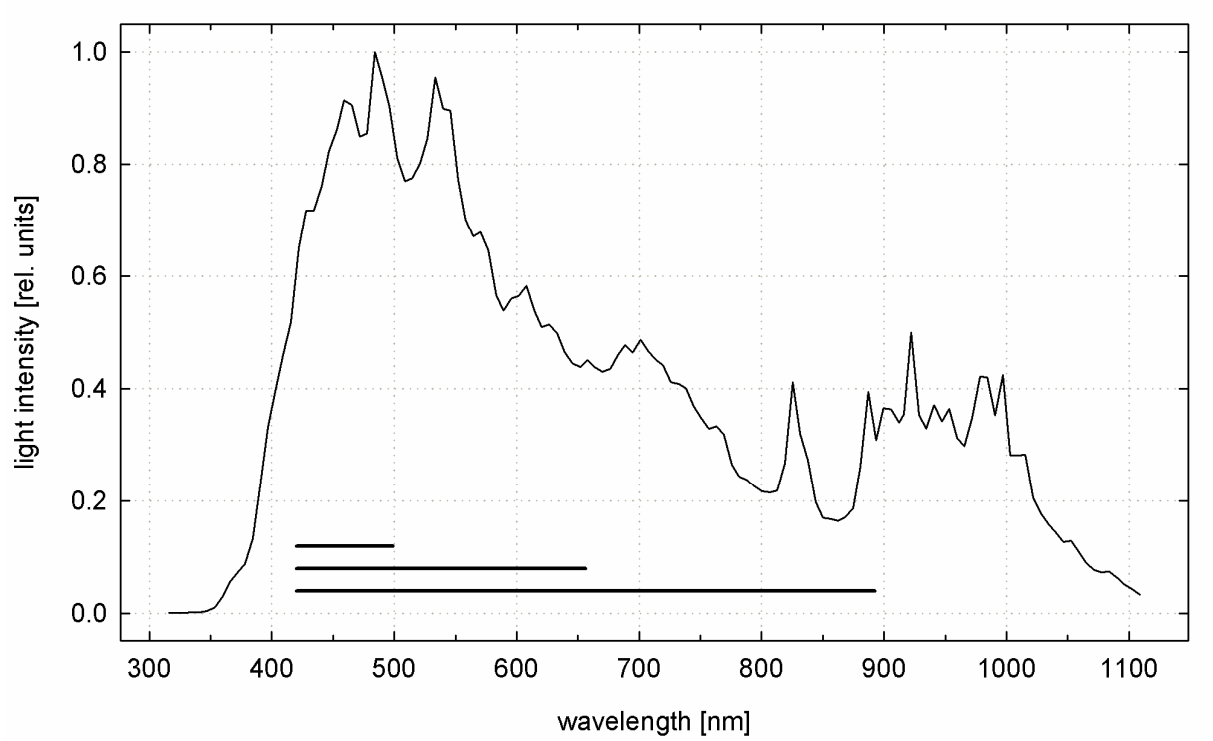

This spectrum was measured by the instrument's intrinsic photodiode array detector and therefore also contains all distortions added by all optical components, monochromator, diffraction grating and detector sensitivity. A diffraction grating with 600 grooves per millimetre was used. The spectral resolution is 6.22 nm per point. Effective measuring range with our current setup is approximately 380 – 1050 nm. In the UV it is limited by the absorption of a lens, which is made of common glass and also by the fibre optic bundles. In the NIR the limit is both low light intensity from the lamp and the absorption limit of the silicon-based photodiode detector.

The three line segments at the bottom of the graph indicate achievable measuring ranges in our current instrument setup. They, from top to bottom, illustrate ranges of the three gratings mounted into the monochromator. The first grating has 1800 grooves per millimetre and ~79 nm wide chunk of spectrum can be measured at the same time. The second grating has 600 grooves per millimetre and ~236 nm wide part of the spectrum can be measured simultaneously. The last grating has 300 grooves per millimetre and enables one to measure a spectrum part ~472 nm wide. The respective resolutions per point are 2.0733, 6.22 and 12.44 nm per point.

VI.5 Properties of diffraction gratings used in our kinetic spectrophotometer

VI.5.1 Grating 1: 1800 lines/mm

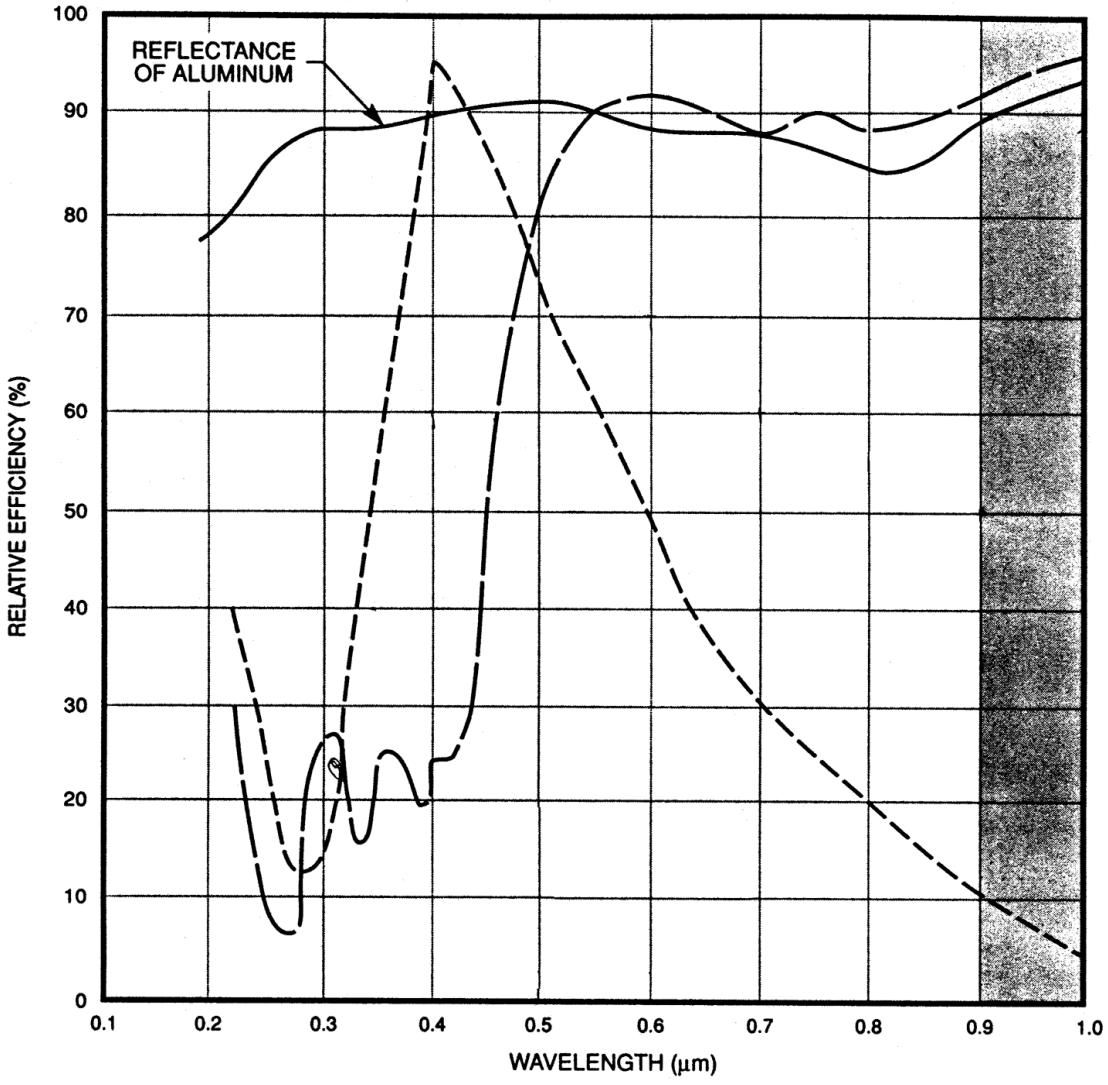

Spectral efficiency of the grating plotted separately for light polarized perpendicular to the grooves (log dash) and parallel to the grooves (short dash). This holographic grating is blazed at 500 nm. We only use this grating in the region 400-700 nm. The image is modified from Oriel Instruments Inc. data.

VI.5.2 Grating 2: 600 lines/mm

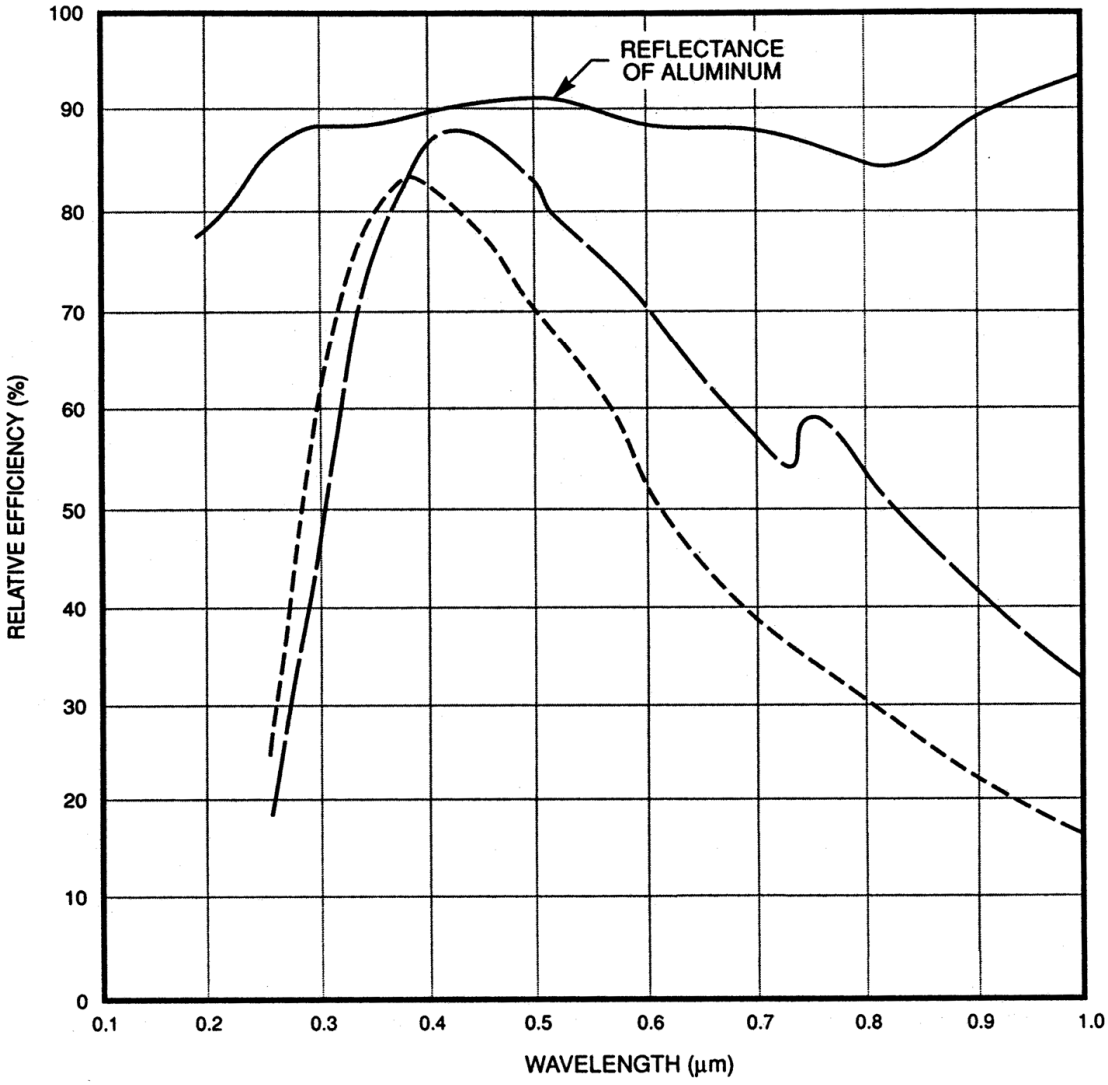

Spectral efficiency of the grating plotted separately for light polarized perpendicular to the grooves (log dash) and parallel to the grooves (short dash). This ruled grating is blazed at 400 nm. The image is modified from Oriel Instruments Inc. data.

VI.5.3 Grating 3: 300 lines/mm

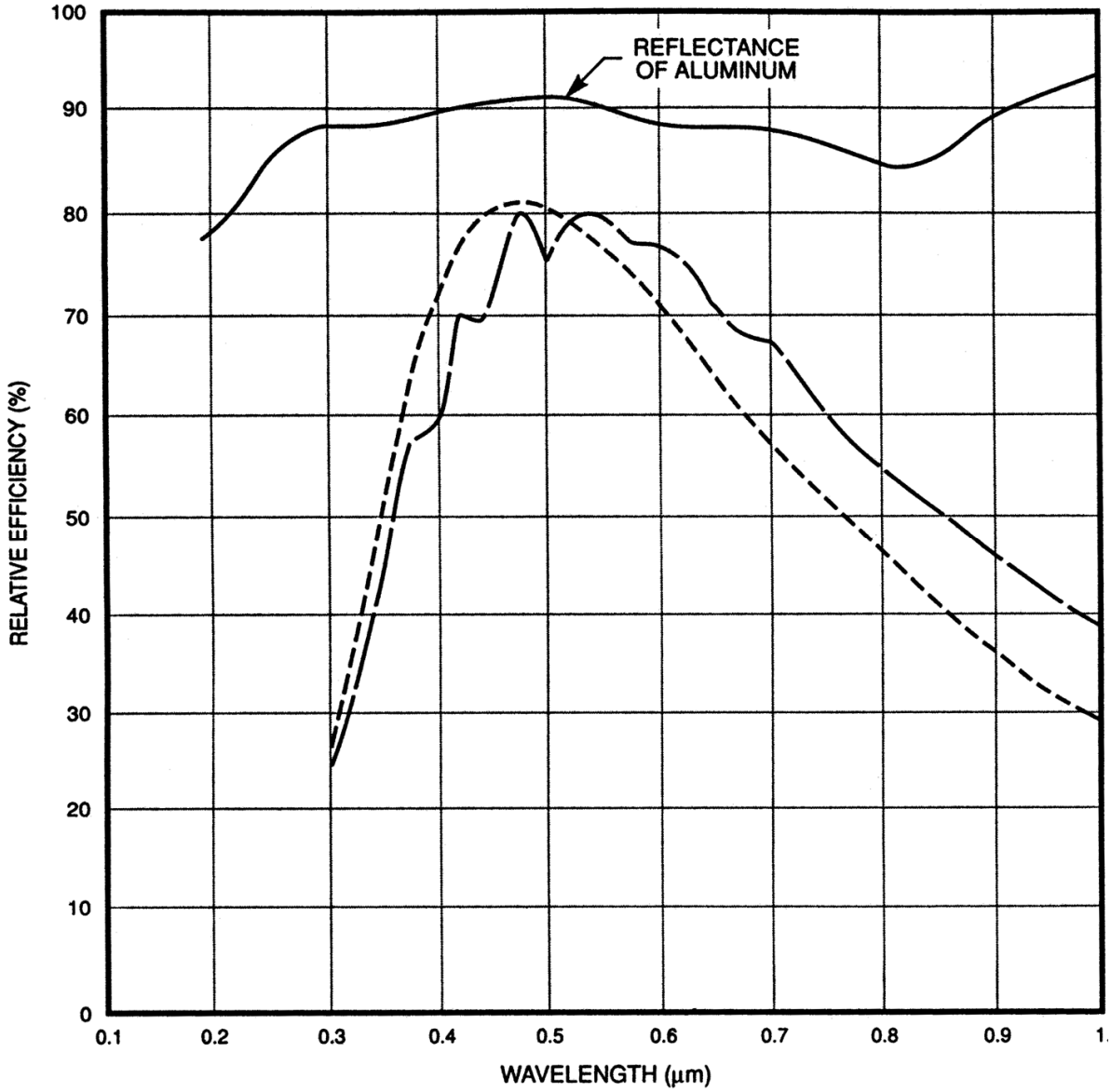

Spectral efficiency of the grating plotted separately for light polarized perpendicular to the grooves (log dash) and parallel to the grooves (short dash). This ruled grating is blazed at 500 nm. The image is modified from Oriel Instruments Inc. data.

VI.6 Electronic shutter speed

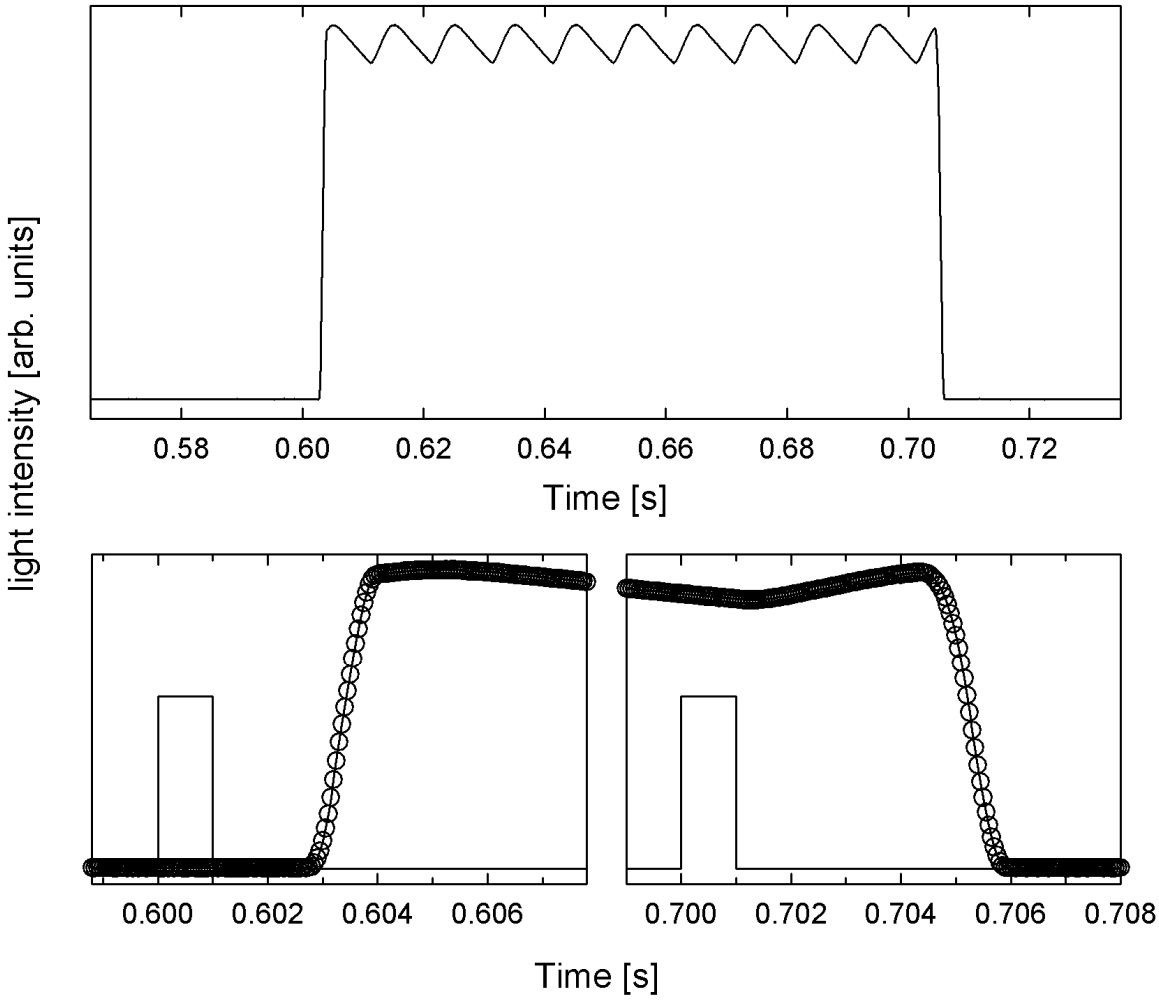

Continuous actinic light is turned on and off by an electronic shutter. Typical shutter operating speeds are demonstrated in this image.

Top panel – overall pattern of shutter usage. Note periodic fluctuations of light output caused by the alternating current flowing through the halogen lamp. Direct current-driven lamp may be advantageous is some settings.

Below-left – detail of the opening of the shutter. Measured light intensity is plotted as continuous line with open circles showing each data point. Rectangular signal sent to the shutter driver is also shown. The shutter is fully opened within three milliseconds after the driving signal finished. The opening itself takes ~1100 µs. 1 ms signal is sufficient to operate the shutter.

Below-right – detail of the shutting down of the shutter. The shutter is fully closed within 5 ms after the driving signal finished. The shutdown itself takes ~1500 µs.

The data for this image were obtained by measuring fluorescence emitted from the chlorophyll extract of hibiscus leaf. The sampling period was 50 µs.

VI.7 Fluorescence spectrum as seen by the absorption spectrophotometer

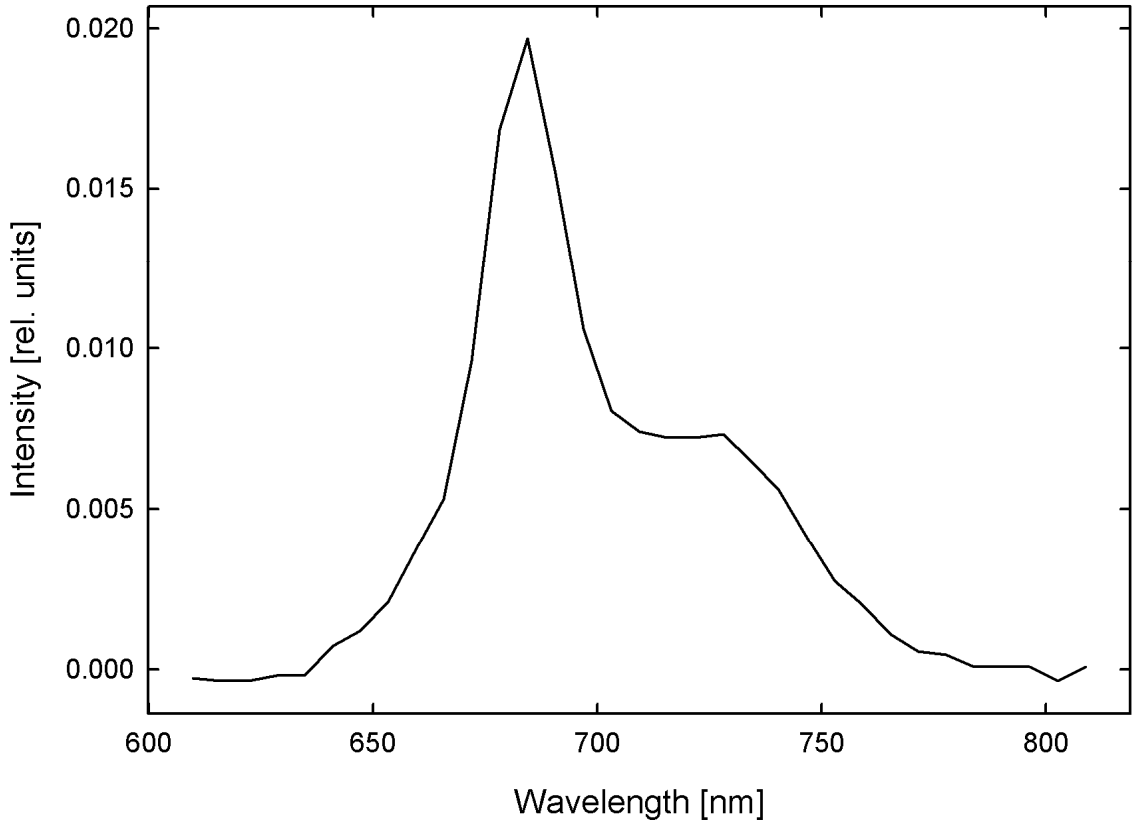

This image shows a relatively nice emission spectrum of a chlorophyll extract from hibiscus leaf measured by our kinetic spectrophotometer (chlorophyll concentration ~40 μg/ml). Very intense Xe lamp flash filtered by a blue filter was used as excitation light. These spectra are routinely collected during experiments which use this Xe lamp as actinic light. A read-out with no measuring flash (probe) is always collected to account for fluorescence and light scattering caused by actinic flashes (pumps). Please note that this image is an example of a best-case scenario, i.e. the sample has high fluorescence yield, high concentration and the excitation pulse is very intense (near-saturating for most photosynthetic samples).